

Possible Phase diagram of Helium 4

Jinwu Ye

Department of Physics, The Pennsylvania State University, University Park, PA, 16802
(December 2, 2024)

The phase diagram of 4He was previously thought to consist of only 3 phases: normal liquid, superfluid and normal solid. However, recent torsional oscillator experiments detected some signatures of a possible new state of matter: supersolid state which has both crystalline and superfluid order. We develop a simple Ginsburg Landau theory to study all the possible phases in 4He from a unified point of view. We use the theory to map out the global phase diagram of 4He , address several important experimental facts and also make some predictions that are amenable to experimental tests. A key prediction is that the X-ray scattering intensity from the SS ought to have an additional modulation over that of the NS. The modulation amplitude is proportional to the Non-Classical Rotational-Inertial (NCRI) observed in the torsional oscillator experiments.

1. Introduction: A solid can not flow. While a superfluid can flow without any resistance. A supersolid (SS) is a new state of matter which has both the solid and superfluid order. The possibility of a supersolid phase in 4He due to very large zero point quantum fluctuations was theoretically speculated in 1970 [1–4]. Over the last 35 years, a number of experiments have been designed to search for the supersolid state without success. However, recently, by using torsional oscillator measurement, a PSU group lead by Chan observed a marked $1 \sim 2\%$ Non-Classical Rotational Inertial (NCRI) of solid 4He at $\sim 0.2K$, both when embedded in Vycor glass [5] and in bulk 4He [6]. The NCRI is a low temperature reduction in the rotational moment of inertia due to the superfluid component of solid 4He [3]. Some of the important experimental facts are: (1) the superfluid fraction has a non-monotonic dependence on the pressure, it increases first, reaches a maximum at ~ 55 bar, then decreases to zero at a much higher pressure $p_u \sim 170$ bar [10]. (2) The supersolid has a very low critical velocity corresponding to $\sim 1 - 3$ flux quanta above which the NCRI is reduced (3) A tiny fraction of 3He will decreases the superfluid fractions, but increases the supersolid to normal solid transition temperature considerably [10]. They mapped out the experimental global phase diagram of 4He in the Fig.4 in [6]

The PSU experiments rekindled extensive theoretical interests in the still controversial supersolid phase of 4He . There are two kinds of complementary theoretical approaches. The first is the microscopic numerical simulation [7]. The second is the phenomenological approach [1,9]. In this paper, assuming there are vacancies even in the ground state [1,2,8], we will address the following two questions from the second approach: (1) How can a supersolid phase naturally fits into the the previously thought 4He phase diagram (2) What is the properties of the supersolid to be tested by possible new experiments. We develop a simple and powerful Ginsburg Landau (GL) theory to map out the 4He phase diagram and study all the phases and phase transitions in a unified framework. The SS phase naturally and consistently fits into

the phase diagram. The theory can be used to address several important phenomena observed in the PSU experiments and also make sharp predictions to be tested by possible future experiments, especially X-ray scattering experiments in the SS state.

2. Ginsburg-Landau theory of 4He : Let's start by reviewing all the known phases in 4He . The density of a normal solid (NS) is defined as $n(\vec{x}) = n_0 + \sum'_{\vec{G}} n_{\vec{G}} e^{i\vec{G}\cdot\vec{x}}$ where $n_{\vec{G}}^* = n_{-\vec{G}}$ and \vec{G} is any non-zero reciprocal lattice vector. In a normal liquid (NL), if the static liquid structure factor $S(k)$ has its first maximum peak at \vec{k}_n , then near $k = k_n$, $S^{-1}(k) \sim r_n + c(k^2 - k_n^2)^2$. If the liquid-solid transition is weakly first order, it is known that the classical free energy to describe the NL-NS transition is [12]:

$$f_n = \sum_{\vec{G}} \frac{1}{2} r_{\vec{G}} |n_{\vec{G}}|^2 - w \sum_{\vec{G}_1, \vec{G}_2, \vec{G}_3} n_{\vec{G}_1} n_{\vec{G}_2} n_{\vec{G}_3} \delta_{\vec{G}_1 + \vec{G}_2 + \vec{G}_3, 0} + u \sum_{\vec{G}_1, \vec{G}_2, \vec{G}_3, \vec{G}_4} n_{\vec{G}_1} n_{\vec{G}_2} n_{\vec{G}_3} n_{\vec{G}_4} \delta_{\vec{G}_1 + \vec{G}_2 + \vec{G}_3 + \vec{G}_4, 0} + \dots \quad (1)$$

where $r_{\vec{G}} = r_n + c(G^2 - k_n^2)^2$ is the tuning parameter controlled by the pressure.

It was known that the Superfluid (SF) to Normal Liquid transition at finite temperature is a 3d XY transition described by:

$$f_\psi = K |\nabla \psi|^2 + t |\psi|^2 + u |\psi|^4 + \dots \quad (2)$$

where ψ is the complex order parameter and t is the tuning parameter controlled by the temperature.

The coupling between $n(\vec{x})$ and $\psi(\vec{x})$ consistent with all the symmetry can be written down as:

$$f_{int} = v_1 n(\vec{x}) |\psi(\vec{x})|^2 + \dots \quad (3)$$

where it is expected that the interactions are repulsive $v_1 > 0$. As shown in section 5, these repulsive interactions are crucial to shift down the supersolid transition temperature in Fig.1.

In an effective GL theory, $n(\vec{x})$ and $\psi(\vec{x})$ emerge as two independent order parameters. The total density of

the system is $n_t(x) = n(x) + |\psi(x)|^2$ where $n(x)$ is the normal density and $|\psi(x)|^2$ is the superfluid density. A NS is defined by $n_{\vec{G}} \neq 0, \langle \psi \rangle = 0$, while a supersolid (SS) is defined by $n_{\vec{G}} \neq 0, \langle \psi \rangle \neq 0$. From the NL side, one can approach both the NS and the SF. Inside the NL, $t > 0$, ψ has a gap, so can be integrated out, we recover the NS-NL transition tuned by $r_{\vec{G}}$ in Eqn.1 (Fig.1). Inside the NL $\langle n(\vec{x}) \rangle = n_0$, so we can set $n_{\vec{G}} = 0$ for $\vec{G} \neq 0$ in Eqn.3, then we recover the NL to SF transition tuned by t in Eqn.2 (Fig.1).

Although the NL-NS and NL-SF transitions are well understood, the SF-NS transition has not been investigated seriously. This transition must be in a completely different universality class than the NL-NS transition, because both sides break two completely different symmetry: internal global $U(1)$ symmetry and translational (and orientational) symmetry. It is certainly possible that the solid reached from the SF side is a new kind of solid than the NS reached from the NL side. In the following, incorporating quantum fluctuations into f_ψ (see Eqn.4) and considering the density-density coupling between ψ and n sector in Eqn.3, we will determine the global phase diagram of 4He .

3. Two-component Quantum GL theory in the ψ sector: In this section, we develop a two-component Quantum GL theory in the ψ sector to replace Eqn.2 to describe the superfluid side of 4He . The superfluid is described by a complex order parameter ψ whose *condensation* leads to the Landau's quasi-particles. Although the bare 4He atoms are strongly interacting, the Landau's quasi-particles are weakly interacting. The dispersion curve of superfluid state is shown in Fig.1 b which has both a phonon sector and a roton sector. In order to focus on the low energy modes, we divide the spectrum into two regimes: the low momenta regime $k < \Lambda$ where there are phonon excitations with linear dispersion and high momentum regime $|k - k_r| < \Lambda \ll k_r$ where there is a roton minimum at the roton surface $k = k_r$. We separate the complex order parameters $\psi(\vec{x}, \tau) = \psi_1(\vec{x}, \tau) + \psi_2(\vec{x}, \tau)$ into $\psi_1(\vec{x}, \tau) = \int_0^\Lambda \frac{d^d k}{(2\pi)^d} e^{i\vec{k} \cdot \vec{x}} \psi(\vec{k}, \tau)$ and $\psi_2(\vec{x}, \tau) = \int_{|k - k_r| < \Lambda} \frac{d^d k}{(2\pi)^d} e^{i\vec{k} \cdot \vec{x}} \psi(\vec{k}, \tau)$ which stand for low energy modes near the origin and k_r respectively. For the notation simplicity, in the following, \int_Λ means $\int_{|k - k_r| < \Lambda}$. The QGL action in the ψ sector in the (\vec{k}, ω) space becomes:

$$\begin{aligned} \mathcal{S}_\psi &= \frac{1}{2} \int_0^\Lambda \frac{d^d k}{(2\pi)^d} \frac{1}{\beta} \sum_{i\omega_n} (\kappa\omega_n^2 + t + Kk^2) |\psi_1(\vec{k}, i\omega_n)|^2 \\ &+ \frac{1}{2} \int_\Lambda \frac{d^d k}{(2\pi)^d} \frac{1}{\beta} \sum_{i\omega_n} (\kappa\omega_n^2 + \Delta_r + v_r(k - k_r)^2) |\psi_2(\vec{k}, i\omega_n)|^2 \\ &+ u \int d^d x d\tau |\psi_1(\vec{x}, \tau) + \psi_2(\vec{x}, \tau)|^4 + \dots \end{aligned} \quad (4)$$

where $t \sim T - T_c$ where $T_c \sim 2.17K$ is the critical tem-

perature of SF to NL transition at $p = 0.05$ bar and $\Delta_r \sim p_c - p$ where $p_c \sim 25$ bar is the critical pressure of SF to the SS transition at $T = 0$. In principle, the terms like $\psi^\dagger \partial_r \psi$ may exist, but they are irrelevant in the SF phase.

4. SF to SS transition and global phase diagram: In the SF state, the Feynman relation between the Landau quasi-particle dispersion relation in the ψ sector and the static structure factor in the n sector holds:

$$\omega(q) = \frac{q^2}{2mS(q)} \quad (5)$$

In the $q \rightarrow 0$ limit, $S(q) \sim q$, $\omega(q) \sim q$ recovers the ψ_1 sector near $q = 0$. The first maximum peak in $S(q)$ corresponds to the roton minimum in $\omega(q)$ in the ψ_2 sector, namely, $k_n = k_r$. As one increases the pressure p , the interaction u also gets bigger and bigger, the first maximum peak of $S(q)$ increases, the roton minimum Δ_r gets smaller and smaller. Across the critical pressure $p = p_c$, there are two possibilities (1) The resulting solid is a commensurate solid where $\langle \psi \rangle = 0$ (2) The resulting solid is an in-commensurate solid with vacancies even at $T = 0$ whose condensation leads to $\langle \psi \rangle \neq 0$ [1,2,8]. Case (1) is trivial, the SS phase in Fig.1 does not exist. In the following, we only focus on case (2). From Eqn.1 and Eqn.4, we can see that n and ψ_2 have very similar propagators, so the lattice formation in n sector with $n(x) = \sum_{\vec{G}} n_{\vec{G}} e^{i\vec{G} \cdot \vec{x}}$ and the density wave formation in ψ_2 sector with $\langle \psi_2(\vec{x}) \rangle = e^{i\theta_2} \sum_{m=1}^P \Delta_m e^{i\vec{Q}_m \cdot \vec{x}}$ where $Q_m = k_r$ happen simultaneously. The ψ_2 sector alone is described by $n = 2$ component $(d+1, d)$ with $d = 3$ Lifshitz action [12]. The repulsive ρ density- n density coupling in Eqn.3 $v_1 > 0$ simply shifts the DW by suitable constants along the three unit vectors in the direct lattice. These constants will be determined in the next section for different n lattices. Namely, the SS state consists of two inter-penetrating lattices formed by the n lattice and the ψ_2 density wave.

Combining the roton condensation picture in this section with the results in section 2, we can sketch the following global phase diagram of ${}^4\text{He}$.

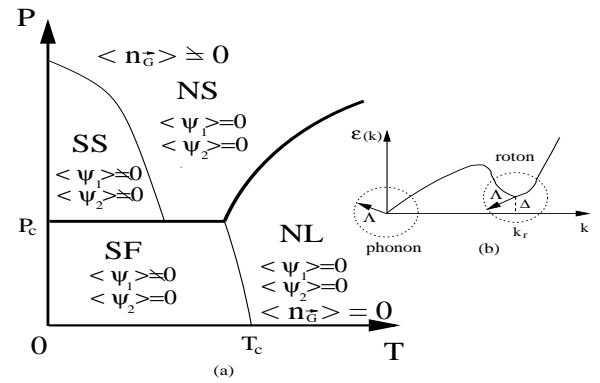


Fig.1: (a) The theoretical phase diagram in the pressure P ver-

sus the temperature T . T controls thermal fluctuations, while P tunes quantum fluctuations. Thick (thin) lines are 1st (2nd) order transitions. The critical temperatures of NL to SF and NS to SS transitions drop slightly as the pressure p increases because of the quantum fluctuations [13]. (b) The separation of low (phonon) and high (roton) momenta regime in the SF. This phase diagram works only when there are vacancies even at $T = 0$.

5. The NS to SS transition: In this section, we approach the SS phase from the NS side and determine its lattice structure. In the NL, the BEC happens in the ψ_1 sector at $k = 0$, ψ_2 has a large gap and can be simply integrated out. In the NS, ψ stands for the vacancies due to large zero point quantum fluctuations [1,2,8]. Due to the lack of particle-hole symmetry in the NS, additional terms like $n(\vec{x})(\psi_1\partial_\tau\psi_1 + \psi_2\partial_\tau\psi_2)$ should exist and is very important at zero temperature and will be investigated in [13]. However, in the classical phase transitions investigated in this paper, this term can still be neglected. Due to the n lattice formation, the mass of ψ_1 was increased to $t_{\psi_1}^{NS} = t + v_1^{NS}n_0 > t_{\psi_1}^{NL} = t + v_1^{NL}n_0$, because we expect $v_1^{NS} > v_1^{NL} > 0$. So the transition temperature T_{SS} from the NS to the SS will *shift down* to a lower temperature $T_{SS} < T_c$ as shown in Fig.1. In the presence of the periodic potential of $n(x)$ lattice, ψ will form a Bloch wave, the u self-interaction in the ψ sector in Eqn.4 will certainly favor extended Bloch wave over strongly localized Wannier state. In principle, a full energy band calculation incorporating the interaction u is necessary to get the energy bands of ψ . Fortunately, qualitatively physical picture can be achieved without such a detailed energy band calculation. In the following, substituting the DW ansatz $\langle\psi_1(\vec{x})\rangle = ae^{i\theta_1}$ and $\langle\psi_2(\vec{x})\rangle = e^{i\theta_2}\sum_{m=1}^P\Delta_m e^{i\vec{Q}_m\cdot\vec{x}}$ where $Q_m = Q$ into Eqn.3, we study the effects of n lattice on $\psi = \psi_1 + \psi_2$. In order to get the lowest energy ground state, we must consider the following 4 conditions: (1) because any complex ψ (up to a global phase) will lead to local supercurrents which is costly, we can also take ψ to be real, so \vec{Q}_m have to be paired as anti-nodal points. P has to be even (2) as shown from the Feynmann relation Eqn.5, $\vec{Q}_m, m = 1, \dots, P$ are simply P shortest reciprocal lattice vectors, then translational symmetry of the lattice dictates that $\epsilon(\vec{K} = 0) = \epsilon(\vec{K} = \vec{Q}_m)$, ψ_1 and ψ_2 have to condense at the same time. (3) The point group symmetry of the lattice dictates $\Delta_m = \Delta$ and is real (4) The strong repulsive interaction $v_1 > 0$ favors $\psi(x = 0) = 0$, so the Superfluid Density Wave (SDW) $\rho = |\psi|^2$ can avoid the n lattice as much as possible. It turns out that the 4 conditions can fix the relative phase and magnitude of ψ_1 and ψ_2 to be $\theta_2 = \theta_1 + \pi, \Delta = a/P$, namely, $\psi = ae^{i\theta}(1 - \frac{2}{P}\sum_{m=1}^{P/2}\cos\vec{Q}_m\cdot\vec{x})$. In this state, the crystal momentum $\vec{k} = 0$ and the Fourier components are $\psi(\vec{K} = 0) = a, \psi(\vec{K} = \vec{Q}_m) = -a/P$ which oscillate in sign and decay in magnitude. In principle, higher Fourier

components may also exist, but they decay very rapidly, so can be neglected without affecting the physics qualitatively. In the following, we will discuss 4 common lattices sc, fcc, bcc, hcp respectively.

(a) $P = 6$: $\vec{Q}_i, i = 1, 2, 3, 4, 5, 6$ are the 6 shortest reciprocal lattice vectors generating a cubic lattice. The maxima of the DW $\psi_{max} = 2a$ appear exactly in the middle of lattice points at the 8 points $\vec{a} = \frac{1}{2}(\pm\vec{a}_1 \pm \vec{a}_2 \pm \vec{a}_3)$. They form the dual lattice of the cubic lattice which is also a cubic lattice.

(b) $P = 8$: $\vec{Q}_i, i = 1, \dots, 8$ form the 8 shortest reciprocal lattice vectors generating a *bcc* reciprocal lattice which corresponds to a *fcc* direct lattice. The field is $\psi(\vec{x}) = a[1 - \frac{1}{4}(\cos\vec{Q}_1\cdot\vec{x} + \cos\vec{Q}_2\cdot\vec{x} + \cos\vec{Q}_3\cdot\vec{x} + \cos\vec{Q}_4\cdot\vec{x})]$, The local superfluid density $\rho_{DW}^l = |\psi(\vec{x})|^2$. The maxima of the DW $\psi_{max} = 2a$ appear in all the edge centers such as $(1/2, 0, 0)$ etc. and the centers of any cube such as $(1/2, 1/2, 1/2)$.

(c) $P = 12$: $\vec{Q}_i, i = 1, \dots, 12$ form the 12 shortest reciprocal lattice vectors generating a *fcc* reciprocal lattice which corresponds to a *bcc* direct lattice. The field is $\psi(\vec{x}) = a[1 - \frac{1}{6}(\cos\vec{Q}_1\cdot\vec{x} + \cos\vec{Q}_2\cdot\vec{x} + \cos\vec{Q}_3\cdot\vec{x} + \cos\vec{Q}_4\cdot\vec{x} + \cos\vec{Q}_5\cdot\vec{x} + \cos\vec{Q}_6\cdot\vec{x})]$. The maxima of the DW $\psi_{max} = 4/3a$ appear along any square surrounding the center of the cube such as $(1/2, \beta, 0)$ or $(1/2, 0, \gamma)$ etc. Note that 4He in Vycor glass takes a *bcc* lattice

(d) Unfortunately, a spherical $k_r = Q$ surface can not lead to lattices with *different* lengths of primitive reciprocal lattice vectors such as a *hcp* lattice. This is similar to the classical liquid-solid transition described by Eqn.1 where a single maximum peak in the static structure factor can not lead to a *hcp* lattice [12]. Here we can simply take the experimental fact that n forms a *hcp* lattice without knowing how to produce such a lattice from a GL theory Eqn.1. Because for an ideal *hcp* lattice $c/a = \sqrt{8/3}$, an *hcp* lattice has 12 nearest neighbours, so its local environment may resemble that of an *fcc* lattice. We expect the physics (except the weak anisotropy of NCRI in the *hcp* lattice discussed in [13]) is qualitatively the same as that in *fcc* direct lattice.

Let's look at the prediction of our theory on X-ray scattering from the SS. For simplicity, we take the *sc* lattice to explain the points. The other lattices will be detailed in [13]. For a lattice with $j = 1, \dots, n$ basis located at \vec{d}_j , the geometrical structure factor at the reciprocal lattice vector \vec{K} is $S(\vec{K}) = \sum_{j=1}^n f_j(\vec{K})e^{i\vec{K}\cdot\vec{d}_j}$ where f_j is the atomic structure factor of the basis at \vec{d}_j . The X-ray scattering amplitude $I(\vec{K}) \sim |S(\vec{K})|^2$. For the SS in the *sc* lattice, $\vec{K} = \frac{2\pi}{a}(n_1\vec{i} + n_2\vec{j} + n_3)\vec{k}, \vec{d}_1 = 0, \vec{d}_2 = \frac{a}{2}(\vec{i} + \vec{j} + \vec{k})$, then $S(\vec{K}) = 1 + f(-1)^{n_1+n_2+n_3}$ where $f \sim \rho_s^{max} \sim a^2$. It is $1 + f$ for even \vec{K} and $1 - f$ for odd \vec{K} . In fact, due to large zero-point motion, any X-ray scattering amplitude $I(\vec{K})$ will be diminished by a Debye-Waller factor. As shown in [13], the lattice phonon modes \vec{u} in ψ are *locked*

to those of n , so there is a *common* Debye-Waller factor $\sim e^{-\frac{1}{3}K^2 \langle u^2 \rangle}$ for both even and odd \vec{K} . We conclude that the *elastic* X-ray scattering intensity from the SS has an additional modulation over that of the NS. The modulation amplitude is proportional to the maxima of the superfluid density $\rho_s^{max} \sim a^2$ which is the same as the NCRI observed in the PSU's torsional oscillator experiments. Unfortunately, so far, the X-ray scattering data is limited to high temperature $T > 0.8K > T_{SS}$ [14]. X-ray scattering experiments on lower temperature $T < T_{SS}$ are needed to test this prediction.

The results achieved in this section indeed confirm Fig.1 achieved from the roton condensation picture in the last section. A low energy effective action involving the superfluid phonon θ , the lattice phonons \vec{u} and their couplings will be discussed in [13].

6. The vortices in the SS: In the sectors of ψ , there are topological defects in the phase winding of θ which are vortices. At $T \ll T_{SS}$, the vortices can only appear in tightly bound pairs. However, as $T \rightarrow T_{SS}^-$, the vortices start to become liberated, this process renders the total NCRI to vanish above $T > T_{SS}$ in the NS state. In the SF phase, a single vortex energy costs a lot of energy $E_v^{SF} = \frac{\rho_s^{SF} h^2}{4\pi m^2} \ln \frac{R}{\xi_{SF}}$ where m is the mass of 4He atom, R is the system size and $\xi_{SF} \sim a$ is the core size of the vortex. This energy determines the critical velocity in SF $v_c^{SF} > 30cm/s$. In the SS state, because in the center of the SS vortex core, $\psi = 0$, so the vortices prefer to sit on a lattice site of the n lattice. Because the long distance behavior of SS is more or less the same as SF, we can estimate its energy $E_v^{SS} = \frac{\rho_s^{SS} h^2}{4\pi m^2} \ln \frac{R}{\xi_{SS}}$. We expect the core size of a supersolid vortex $\xi_{SS} \sim 1/\Lambda \gg 1/k_r \sim a \sim \xi_{SF}$. so inside the SS vortex core, we should also see the lattice structure of n . In fact, we expect that ξ_{SS} is of the order of the average spacing between vacancies. It is interesting to see if neutron or light scattering experiments can test this prediction. Compared to E_v^{SF} , there are two reductions, one is the superfluid density, another is the increase of the vortex core size $\xi_{SS} \gg \xi_{SF}$. These two factors contribute to the very low critical velocity $v_c^{SS} \sim 30\mu m/s$.

7. Discussions on PSU's experiments: Although the NS to SS transition is in the same universality class as the NL to SF one [9], it may have quite different off-critical behaviours due to the DW structure in the SS state. We can estimate the critical regime of the NS to SS transition from the Ginsburg Criterion $t_G^{-1} \sim \xi_{SS}^3 \Delta C$ where ΔC is the specific jump in the mean field theory. Because of the cubic dependence on ξ_{SS} , large ξ_{SS} leads to extremely narrow critical regime, the 3D XY critical behavior is essentially irrelevant, instead mean field Gaussian theory should apply. Assuming 3He impurities diffusion process is slow: this fact can be used to address two experimental observations related to their effects: (1) The unbinding transition temperature T_{SS}

is determined by the pinning due to impurities instead of by the logarithmic interactions between the vortices which is proportional to the superfluid stiffness. So the 3He impurities effectively pin the vortices and raise the unbinding critical temperature T_{SS} . On the other hand, 3He impurities will certainly decrease the superfluid density in both the ψ_1 and ψ_2 sector just like 3He impurities decreases superfluid density in the 4He superfluid. (2) The mean field jump will certainly be smeared by the presence of 3He impurities. So we expect that the λ peak will be smeared in the specific heat measurement near $T = T_{SS}$.

8. Conclusions: The QGL theory developed in this paper leads to a global and unified picture of 4He physics at any temperature and pressure. Assuming there are vacancies even in the ground state, we investigate the SS state from both the SF and the NS side and find completely consistent description of the properties of the SS state. We found that the SF to the SS transition is a first order transition driven by the collapsing of roton minimum in the SF side, while the NS to SS transition is described by a 3d XY model with much *narrower* critical regime than the NL to SF transition. The size of a supersolid vortex core is much larger than that of a superfluid vortex core. These facts are responsible for the smearing of specific anomaly and the extremely sensitivity to even tiny concentrations of 3He impurities. The SS state is a uniform two-component phase consisting of a normal lattice plus a commensurate superfluid density wave (SDW). The SDW in the SS state leads to a modulation on the X-ray scattering intensity over that of the NS. The modulation amplitude is proportional to the NCRI observed in the PSU's torsional oscillator experiments.

Acknowledgement

I am deeply indebted to Tom Lubensky for many insightful and critical comments on the manuscript. I thank P. W. Anderson, T. Clark, M. Cole, D. Huse, J. K. Jain, G. D. Mahan, especially Moses Chan for helpful discussions. The research at KITP was supported by the NSF grant No. PHY99-07949.

- [1] A. Andreev and I. Lifshitz, Sov. Phys. JETP **29**, 1107 (1969).
- [2] G. V. Chester, Phys. Rev. A **2**, 256 (1970).
- [3] A. J. Leggett, Phys. Rev. Lett. **25**, 1543 (1970).
- [4] W. M. Saslow , Phys. Rev. Lett. **36**, 1151-1154 (1976).
- [5] E. Kim and M. H. W. Chan, Nature **427**, 225 - 227 (15 Jan 2004).
- [6] E. Kim and M. H. W. Chan, Science 24 September 2004; 305: 1941-1944.
- [7] D. M. Ceperley, B. Bernu, Phys. Rev. Lett. **93**, 155303 (2004); N. Prokof'ev, B. Svistunov, *ibid.* **94**, 155302

(2005); D. E. Galli, M. Rossi, L. Reatto, Phys. Rev. B 71, 140506(R) (2005)

[8] P. W. Anderson, W. F. Brinkman, David A. Huse, Science 18 Nov. 2005;310: 1164-1166.

[9] A. T. Dorsey, P. M. Goldbart, J. Toner, Phys. Rev. Lett. **96**, 055301 (2006).

[10] M. Chan, private communications.

[11] T. Schneider and C. P. Enz, Phys. Rev. Lett. 27, 1186?1188 (1971); Yves Pomeau and Sergio Rica , Phys. Rev. Lett. 72, 2426?2429 (1994). P. Nozieres, J. Low Temp. Phys. 137, 45 (2004).

[12] For discussions on Classical Lifshitz Point (CLP) and their applications in nematic to smectic-A and -C transitions in liquid crystal, see the wonderful book by P. M. Chaikin and T. C. Lubensky, principles of condensed matter physics, Cambridge university press,1995.

[13] Jinwu Ye, unpublished.

[14] B. A. Fraass, P. R. Granfors, and R. O. Simmons, Phys. Rev. B 39, 124C131 (1989). C. A. Burns and E. D. Isaacs, Phys. Rev. B 55, 5767C5771 (1997).